Light scattering near the nematic–smectic-A liquid-crystal phase transition

M. E. Lewis, I. Khan, H. Vithana, Alan Baldwin, and D. L. Johnson
Department of Physics, Kent State University, Kent, Ohio 44242

M. E. Neubert
Liquid Crystal Institute, Kent State University, Kent, Ohio 44242
(Received 8 February 1988)

We report the results of light scattering on liquid-crystal materials near the nematic–smectic-A phase transition. Measurements were made both in the nematic and smectic-A phases. The critical exponents for the twist elastic coefficient (K_2) and the layer dilation elastic coefficient ($\bar{B}$) were measured and appear to scale, within experimental uncertainty, as predicted by the de Gennes model. The exponents for these relatively wider nematic range materials are somewhat larger than those found in most previous light scattering studies, indicating somewhat better agreement with the theoretically predicted values for the isotropic 3D XY model, though still considerably smaller.

I. INTRODUCTION

The physics of the nematic to smectic-A (NA) phase transition continues to elude both theorists and experimentalists after more than ten years of intense study. Nevertheless, it remains a premier problem of statistical physics because of two specific features; the fluctuation destruction of long-range smectic order (the smectic-A phase is at the lower critical dimension) and the coupling between the smectic order parameter and the nematic director. The latter makes the problem imperfectly analogous to the gauge invariant Ginzburg-Landau model of superconductivity; unlike the superconductor problem it does not exhibit true gauge invariance but rather global rotational invariance.

The fluctuation destruction of long-range order of the smectic density wave has motivated defect mediated melting models by Helfrich (H),[1] Nelson and Toner (NT),[2] and Dasgupta and Halperin (DH).[3–5] These models are extensions of the original de Gennes model[6] to include thermally generated edge and screw dislocation fields. H and DH predict isotropic inverted 3D XY critical behavior ($\nu_\parallel=\nu_\perp\sim\frac{2}{3}$, $\alpha\sim-0.01$) whereas NT predict highly anisotropic critical exponents, $2\nu_\perp=\nu_\parallel$, but have not calculated actual values. Lubensky[7] has argued that the above two classes of predictions are the only possibilities in the context of de Gennes's model.

Experimentally there is little agreement with theory. The most serious disagreement is the weak anisotropy of the exponents for the nematic twist (K_2) and bend (K_3) elastic coefficients which scale in the de Gennes model as

$$\delta K_2\sim\xi_\perp^2/\xi_\parallel\sim t^{-\rho_2}, \tag{1a}$$

where

$$\rho_2=2\nu_\perp-\nu_\parallel \tag{1b}$$

and

$$\delta K_3\sim\xi_\parallel-t^{-\rho_3}, \tag{2a}$$

where

$$\rho_3=\nu_\parallel . \tag{2b}$$

Here theory predicts that either $\rho_2=\rho_3\sim\frac{2}{3}$ (inverted XY model) or $\rho_2=0$, $\rho_3>0$ (anisotropic models). Experimentally there is not a clear consensus on the absolute values of ρ_2 and ρ_3; however, it is clear that $\rho_2\neq0$ (Ref. 8) and $\rho_3\neq\rho_2$.[8–10] This rules out both the isotropic and anisotropic de Gennes models if the asymptotic regime is accessed experimentally ($5\times10^{-6}\lesssim t_{\text{expt}}\lesssim10^{-2}$), an important caveat given the proximity of tricriticality of the NA phase transition.

The most likely point of agreement is $\rho_3\sim\frac{2}{3}$ which has been shown recently for several materials both polar and nonpolar.[9] However, there is not experimental consensus on this value of ρ_3.[9,10]

The predicted scaling relations Eqs. (1) and (2) for the nematic elastic coefficients have smectic analogs. The smectic elastic coefficients for layer dilation ($\bar{B}$) and for the tilt of the director relative to the layers (D) are predicted to scale as

$$\bar{B}\sim\xi_\parallel'/(\xi_\perp')^2\sim|t|^{\phi}, \tag{3a}$$

where

$$\phi=2\nu_\perp-\nu_\parallel \tag{3b}$$

and

$$D\sim1/\xi_\parallel'\sim|t|^{\phi'}, \tag{4a}$$

where

$$\phi'=\nu_\parallel . \tag{4b}$$

Therefore, theory predicts that either $\phi=\phi'\sim\frac{2}{3}$ (inverted XY model) or $\phi=0$, $\phi'>0$ (anisotropic models). Experimentally it has been reported[11–14] that $\phi\sim\frac{1}{3}$ and $\phi'\sim\frac{1}{2}$, in strong conflict with theory. However, the results of a surface light scattering experiment by Fisch *et al.*[15] on a binary mixture of polar smectic homologs exhibiting

reentrant nematic behavior are consistent with $\phi=0$ near the reentrant concentration. (See, however, Ref. 16.)

In addition to the question of the absolute values of the exponents, $\rho_2,\rho_3;\phi,\phi'$, one can ask whether the scaling laws themselves, expressed in Eqs. (1a), (2a), (3a), and (4a), are valid, i.e., do the relationships

$$\rho_2=\phi \tag{5a}$$

and

$$\rho_3=\phi' \tag{5b}$$

hold experimentally. The latter of these (5b) is clearly negated by current experimental results (see Table I), but again the caveat concerning asymptotia and tricriticality should be heeded. The former (5a) may or may not hold (see the wide range of experimental values in Table I).

One of the two central purposes of this research is to provide the first clear experimental test of Eq. (5a). For this purpose, we chose a material having a relatively wide nematic range (4-*n*-hexyloxybenzoate, $\bar{6}$O9); thus reducing the potential influence of tricriticality.

Specifically we have studied the vanishing of the smectic layer dilation coefficient $\bar{B}$ on approach to T_c from below using a mode-one quasielastic light scattering experiment, and the divergence of the nematic twist coefficient, K_2 on approach to T_c from above using a mode-two quasielastic light scattering experiment. In the context of de Gennes's model these experiments measure ϕ and ρ_2, respectively, and provide the first stringent test of the scaling relation ($\bar{B}^{-1}\sim\delta K_2$) implied by Eqs. (1a) and (3a) and expressed explicitly by Eq. (5a).

The second purpose of this research was to make the first small-angle, high-resolution, *pure-twist mode* ($q_\parallel=0$) light scattering measurements of ρ_2. Previous experiments designed to measure ρ_2 suffered one of two shortcomings: (1) the data analysis required a certain assumption about nonhydrodynamic mode ($q\xi>1$) behavior[25] or (2) the scattering was in the hydrodynamic regime but did not probe pure twist due to a small but not negligible bend contribution ($q_\parallel\neq0$) (Ref. 8), correction for which required the use of x-ray data. Comparison of these two schemes for measuring ρ_2 is given in Table I for 80CB and $\bar{8}$S5. The results are quite different for the two classes of experiments; however, due to the rather large error bars involved in the nonhydrodynamic experiment[10] the values do overlap. Clearly there is a need for small-angle (hydrodynamic-regime) pure-twist mode ($q_\parallel=0$) light scattering measurements of ρ_2, and for a comparison of such measurements with high resolution measurements of ϕ to test the scaling relation [Eqs. (1) and (3)].

II. EXPERIMENTAL PROCEDURES

We refer to the two samples studied as the $\bar{B}$ and K_2 samples in all that follows.

A. Sample preparation and temperature control

Both samples were purified and subsequently analyzed by high-pressure liquid chromatography (HPLC). Their purities by HPLC area ratio analysis were found to be in excess of 99.99%, a great improvement over the standard recrystallization technique. Both samples were confined between 1 in.$\times$1 in.$\times$1 mm glass plates separated by wire spacers and mechanically stabilized by epoxy (Torr

TABLE I. Lists of all the previously reported critical exponents for $K_2(\rho_2)$, $\bar{B}(\phi)$, $K_3(\rho_3)$, and $D(\phi')$ of which we are aware for materials covering the currently accessible range of values of T_{NA}/T_{NI}. It also reports our present measurements of ρ_2 and ϕ for $\bar{6}$O9.

	ρ_2	ϕ	ρ_3	ϕ'	T_{NA}/T_{NI}
CBBOA	0.47±0.07[a]	0.33±0.05[b]	0.65±0.05[c]	0.50±0.02[b]	0.94[c]
			0.74±0.04[d]		
80CB	0.35±0.05[e]	0.33±0.04[g]	0.67±0.05[j]	0.50±0.05[j]	0.96[k]
	0.47±0.11[f]	0.29±0.02[h]	0.75±0.04[f]		
		0.26±0.08[i]	0.66±0.04[l]		
8CB	0.34±0.13[f]	0.26±0.06[l]	0.72±0.05[f]		0.977[m]
			0.62±0.03[l]		
40.8		0.32±0.02[n]	0.69±0.03[n]	0.54±0.04[n]	0.96[k]
		0.44±0.04[o]			
$\bar{8}$S5	0.37±0.06[e]	0.44±0.02[o]	0.68±0.03[j]		0.94[j]
	0.57±0.13[f]		0.89±0.05[f]		
$\bar{6}$O9	0.46±0.03[p]	0.44±0.05[q]	0.66±0.02[j]		0.93[e]
	0.48±0.03[j]				

[a]Reference 17.
[b]Reference 11.
[c]Reference 18.
[d]Reference 19.
[e]Reference 8.
[f]Reference 10.
[g]Reference 20.
[h]Reference 16.
[i]Reference 12.
[j]Reference 9.
[k]Reference 21.
[l]Reference 14.
[m]Reference 22.
[n]Reference 13.
[o]Reference 15.
[p]Reference 23.
[q]Reference 24.

Seal). The thickness of the $\bar{B}$ and K_2 samples, respectively, were nominally 125 and 250μ m. They were, respectively, homogeneously (SiO_x evaporation at $\sim 30°$ from the plane of the substrate) and homeotropically (organosilane surfactant) aligned. Their T_c drifts during the time of data collection were -1.0 and -0.25 mK/day, respectively. The temperature profile in the region of the circular optical port had circular symmetry and was accurately measured to be $T(r)-T(0)=0.4r^2$ mK, where r is measured in mm. The beam waist of the focused He-Ne laser beam (~ 1 mw) was approximately 100 μ for both experiments and was placed as close as possible to the center of the temperature gradient profile. We estimate the temperature variation across the scattering volume to be less than 50 μK. For the $\bar{B}$ experiment the beam (~ 0.8 mm) was expanded ($\times 10$) and focused by a 100-cm focal-length lens whereas for the K_2 experiment the beam was not expanded but was focused by a 10-cm focal-length lens. Temperature control for the $\bar{B}$ experiment was ± 100 μK and for the K_2 experiment ± 250 μK peak to peak. Laser-beam heating of the scattering volume was negligible.

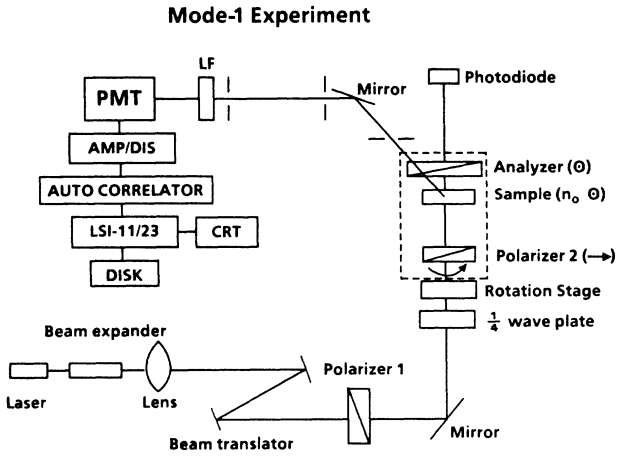

FIG. 1. Schematic diagram of the $\bar{B}$ experiment (mode 1). The element labeled LF is a 6328-Å laser line filter (interference filter). Polarizer 1 and the 1/4λ plate combine to give circularly polarized light. The rotation stage rotates everything inside the dashed line about the laser beam.

B. Light scattering experiments

As mentioned in the Introduction the $\bar{B}$ and K_2 experiments require mode-one and mode-two quasielastic light scattering geometries, respectively. We discuss these experiments separately below.

$\bar{B}$ experiment (mode 1). This class of liquid-crystal homodyne light scattering experiment was first performed by Birecki *et al.*[11] more than a decade ago but only a few experiments like it[12–14] have been performed. It is a difficult experiment because of the stringent requirements on sample alignment. That is, the low light scattering levels of the smectic-A phase can result in mixing of homodyne and heterodyne signals in the presence of static scattering by the easily formed focal conic distortions and defects, which can also induce mode mixing and other spurious effects. Evidence of static director distortion was found in some samples from the beginning and all eventually succumbed to it when attempts were made to collect data than a few tenths of a degree below the transition.

The experimental geometry and hardware are shown schematically in Fig. 1. In this mode-1 geometry the scattered light intensity and relaxation time are given by

$$I^{-1}\sim[K_1q_\perp^2+\bar{B}(q_\parallel/q_\perp)^2]/\epsilon_a^2kT \tag{6}$$

and

$$\tau_1^{-1}=[K_1q_\perp^2+\bar{B}(q_\parallel/q_\perp)^2]/\eta_1\,, \tag{7}$$

respectively, for $q_\parallel/q_\perp \ll 1$. $q_\parallel$ and $q_\perp$ are the components of the scattered wave vector parallel and perpendicular to the nematic director, $\hat{n}_0$. K_1 is the splay elastic coefficient ($\sim 10^{-6}$ dyn), $\bar{B}$ is the smectic-A layer dilation coefficient ($\sim 10^8$ dyn/cm^2 well below T_c) of interest in this experiment [see Eq. (3)], ϵ_a is the optical frequency dielectric anisotropy, η_1 is the mode-1 viscosity, and k is Boltzmann's constant. The internal scattering angle θ is chosen such that q is perpendicular to k_{in}, which for the refractive indices of 6O9 means $\theta=22.4°$. $q_\parallel=0$ in this geometry whereas from Eq. (6) we see that $\bar{B}$ only contributes when $q_\parallel\neq 0$, otherwise one has only a pure splay layer undulation mode contributing to the scattering process. By rotating the polarizer, analyzer, and sample about the beam axis one can bring in the $\bar{B}$ term which quickly dominates because of the largeness of $\bar{B}$ compared to $K_1q_\perp^2$. For small rotations ($\pm\sim 1.5°$) the geometry remains mode 1 to first order and a sharp parabola in I^{-1} versus $q_\parallel/q_\perp$ is generated. From the slope and intercept of I^{-1} versus $(q_\parallel/q_\perp)^2$ one gets $\bar{B}$ and $K_1q_\perp^2$, respectively, [see Fig. (2)] to within a weakly temperature-dependent factor proportional to $(\epsilon_a^2/kT)^{-1}$, which we can take to be constant over the

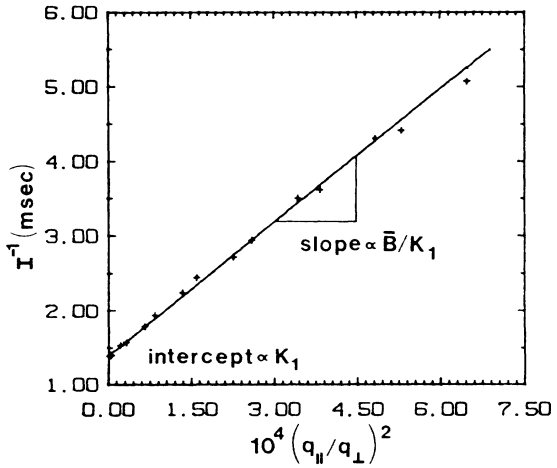

FIG. 2. Plot of parabola data showing the determination of $\bar{B}/K_1$ and K_1 from the intensity data.

narrow range of temperatures probed. We know this to be a very accurate approximation from our auxiliary measurements of n_e and n_0. From the slope and intercept of I^{-1} versus $(q_\parallel/q_\perp)^2$ one gets $\bar{B}/\eta_1$, and $K_1 q_\perp^2/\eta_1$, respectively. τI^{-1} gives η_1, again to within a factor proportional to $(\epsilon_a^2 kT)^{-1}$. This small-angle rotation experiment is in principle very effective in measuring smectic-A viscoelastic properties. We discuss the results of these measurements in the following section.

K_2 experiment (mode 2). This class of high-resolution small-angle mode-two light scattering experiment was first performed in this laboratory by Mahmood *et al.*[8] and Gooden *et al.*[9] in recent years. There had been an earlier lower resolution experiment by Delaye *et al.*[26] and a somewhat higher resolution experiment by Chu and McMillan.[17] The K_2 experiment is as difficult as the $\bar{B}$ experiment but for a different reason. Here the problem is that, unlike the smectic-A elastic constants, there exists a background contribution to the nematic elastic constants; furthermore, for K_2 $(=K_2^0+\delta K_2)$ the background term is relatively much larger than for the bend coefficient, K_3 $(=K_3^0+\delta K_3)$. That is

$$\delta K_2/\delta K_3=(\xi_\perp^0/\xi_\parallel^0)^2 t^{\rho_3-\rho_2},$$

where $\xi_\perp^0, \xi_\parallel^0$ are the bare correlation lengths for order fluctuations perpendicular and parallel to the nematic director respectively. From x-ray scattering experiments[27] we know that $\xi_\perp^0/\xi_\parallel^0 \sim 8-9$ for $\bar{6}O9$; thus the amplitude of the twist singularity is less than 2% of that of the bend singularity. Furthermore $\rho_3 > \rho_2$ for $\bar{6}O9$ which makes this problem even more difficult, requiring data very near T_c.

The experimental geometry and hardware are shown schematically in Fig. 3. In the mode-2 geometry shown, the scattered light intensity and relaxation time are given by

$$I^{-1} \sim K_2 q_\perp^2/\epsilon_a^2 kT \tag{8}$$

and

$$\tau_2=\gamma_1/K_2 q_\perp^2, \tag{9}$$

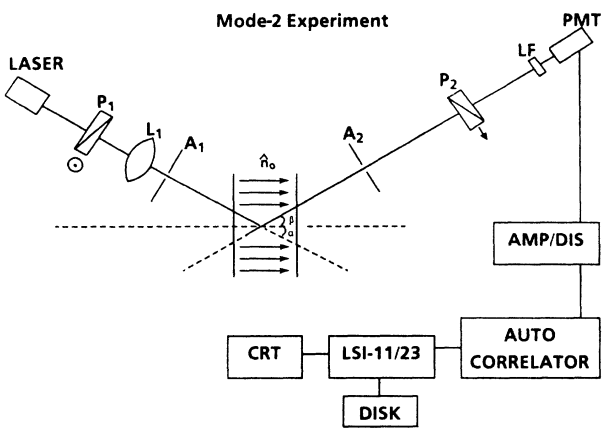

FIG. 3. Schematic diagram of the K_2 experiment (mode 2). The element labeled LF is a laser line filter (interference filter).

where γ_1 is the twist viscosity and the $K_3 q_\parallel^2$ term does not appear because $q_\parallel=0$ when the internal angles α and β are properly chosen. For the refractive indices of $\bar{6}O9$ $\alpha=2.84°$ and $\beta=3.1°$ gives $q_\parallel=0$. Note that the scattering angle is small which means that $q_\perp$ $(1.534\times10^4$ Å$^{-1})$ is also small and the nonhydrodynamic regime correspondingly narrow. We find no evidence of nonhydrodynamic behavior and believe it to be important only well within 1 mK of T_c.

From Eq. (8) it is clear that the temperature dependence of I^{-1} and K_2 should be the same to within a nearly temperature-independent factor $q_\perp^2/\epsilon_a^2 kT$. As in the $\bar{B}$ experiment we are able to show from refractive index measurements that taking $I^{-1} \sim K_2$ is a very accurate approximation. Equations (8) and (9) also imply that $I^{-1}\tau_2 \sim \gamma_1$ to within the same approximation. Thus the K_2 experiment gives very accurately the temperature dependence of K_2 and γ_1.

Photon counting. Both the $\bar{B}$ and K_2 experiments were designed as digital homodyne experiments which means that the photocount correlation function , $C(t)$, is

$$C(t)=\langle n(0)n(t)\rangle=\langle n(0)\rangle^2[1+F(a)e^{-2t/\tau}], \tag{10}$$

where $n(t)$ is the number of photons detected in some time δt $(\ll\tau)$ which is the interval of time each channel of the correlator is kept open before incrementing to the next channel. $\langle n(0)\rangle$ is the average number of photons detected in the time δt and is related to the scattered light intensity by $\langle n(0)\rangle=\sigma I \delta t$, where σ is the quantum efficiency of the photomultiplier tube (EMI 9863 B/100). $F(A)$ is a geometric factor related to the coherence properties of the scattered light, and τ is given by Eqs. (7) and (9) for the $\bar{B}$ and K_2 experiment, respectively.

As pointed out above there is always the risk of a heterodyne contribution in experiments such as these where the dynamic light scattering levels are low and static scattering from sample distortions are a possibility. If such a contribution were present, Eq. (10) would not accurately represent the measured correlation function which would contain an additional term $\sim e^{-t/\tau}$ from the heterodyne signal. If, however, the heterodyne contribution were small, Eq. (10) may still give a good fit of the data but with errors in the parameters $\langle n(0)\rangle$, $F(A)$, and τ. Since $F(A)$ is just a geometrical constant, the constancy of its fitted values provides a check, along with the goodness of fit criterion (χ^2), of the adequacy of Eq. (10) in representing the measured correlation functions. More about this is discussed in the following section.

A home-made 10 ns/channel (δt), one-bit, 128+16 channel autocorrelator was used in the $\bar{B}$ experiment. The 16 delay channels were delayed by 1000 channels to check the constancy of the baseline. The director relaxation times in the smectic-A phase ranged from 50 to 200 μsec so the actual channel times (δt) used were ~ 4 μsec. The average photon count per channel was ~ 0.03 so the correlator measured the full, unclipped correlation function in spite of the fact that the channels were only one bit deep.

III. RESULTS

The $\bar{B}$ experiment. Graphs showing the correlation function geometric factor $F(A)$, the pure splay angle position ($q_{\parallel}=0$), K_1, and K_1/η_1 versus reduced temperature are shown in Figs. 4–7. In all cases the parameters are very stable, being essentially constant for the temperature range of interest. A lack of stability in $F(A)$ would indicate a problem with the optics or sample. The stability of the pure splay angle position reflects the stability of the director alignment, i.e., if the alignment is of high quality and if no defects enter into the scattering volume, the direction of the director should remain constant and the splay position should not change. The stability of K_1 (Fig. 6) and K_1/η_1 (Fig. 7) imply that the main temperature dependence is indeed in the term $\bar{B}/(q_{\parallel}/q_{\perp})^2$ in Eqs. (6) and (7).

Figure 8 is an overlay of the inverse intensity and the inverse relaxation time data for a cooling (C) and a heating (H) run. The intensity and the relaxation time data sets agree quite well with each other. Figures 9 and 10 are linear and log-log plots, respectively, of the data with the best-fit curve drawn through each. The exponent for $\bar{B}$, given in Table I (0.44 ± 0.05) was arrived at by considering the results of range shrinking (~ 0.6 decade) of the fitted data. The heating run had a slightly lower (~ 0.04) exponent for both the relaxation time and the intensity than did the cooling run. This difference, included within the reported error bars, is somewhat disturbing. It may be due to the different surface and/or defect configuration for the cooling and heating runs. A sudden decrease in the transition temperature accompanied by a sudden change in the pure splay position ($q_{\parallel}=0$) was observed during some cooling runs. This is an intrinsic problem with this experiment and may be related to the sudden appearance of focal conic defects.

Figure 11 is an expanded composite graph of the relaxation and intensity data. Notice that in both cases the transition temperature is slightly lower for the inverse relaxation time data. Below about 40.29 °C the intensity and relaxation time data coincide quite well, but the relaxation data are consistently lower near T_c. During the analysis a number of effects which might have caused this were considered, but no satisfactory explanation was found.

The value reported here for the exponent for $\bar{B}$, $\phi=0.44\pm0.05$, is similar to those reported by Fisch *et al.*[15] who performed a surface scattering measurement on 8S5 and 40.8. They reported 0.44 ± 0.04 for both materials. Other reported exponents range from 0.28 and 0.33 (see Table I). It is curious that van Känel *et al.* mea-

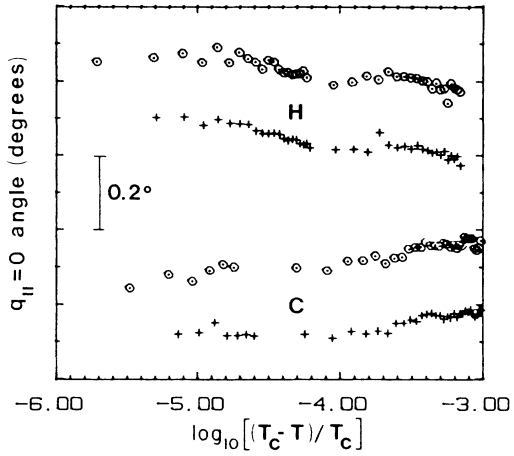

FIG. 5. $q_{\parallel}=0$ (pure splay mode) position degrees vs the log of reduced temperature. The data labeled with ⊙ are inverse relaxation time data. The data labeled with + are inverse intensity data. The lower curves labeled C are from the cooling run and the upper two curves labeled H are from the heating run. If the data were not shifted for clarity, all four data sets would overlay to within 0.2°.

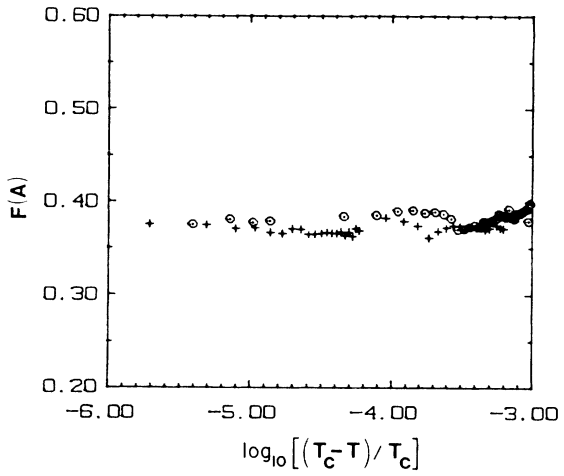

FIG. 4. Geometric factor $F(A)$ vs the log of reduced temperature. The data labeled with ⊙ are from the heating run while the data labeled with + are the cooling run.

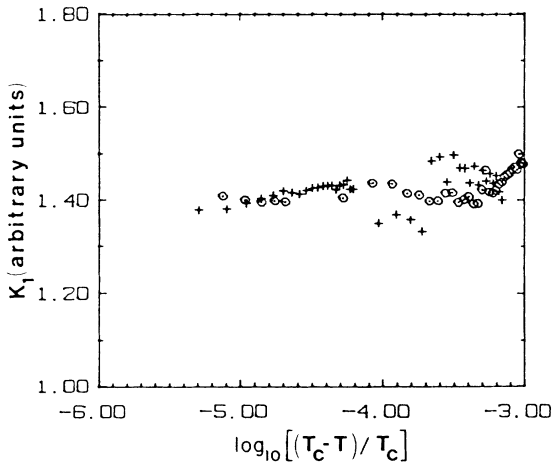

FIG. 6. K_1 vs the log of the reduced temperature. The data labeled with ⊙ are from the cooling run while the data labeled with + are from the heating run.

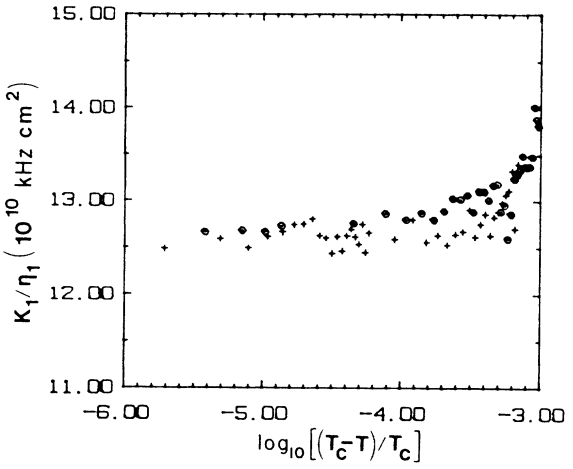

FIG. 7. K_1/η_1 vs the log of reduced temperature. The data labeled with ⊙ are from the cooling run while the data labeled with + are from the heating run.

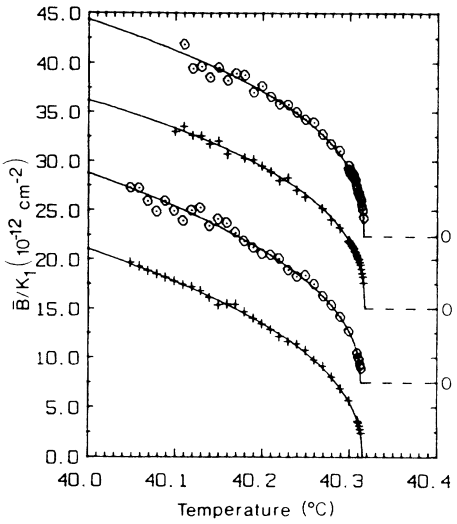

FIG. 9. $\bar{B}/K_1$ vs temperature. Fitted curves are drawn through each. The data have been shifted to separate the curves. The data labeled ⊙ are inverse relaxation time data. The data labeled + are inverse intensity data. The lower two curves are from the cooling run while the upper two curves are from the heating run. The upper three curves are shifted 7.5, 15, and 22.5 units, respectively.

sured a substantially smaller exponent (0.32) (see Table I) for 40.8 with a light scattering measurement similar to the one presented here. All measured values are significantly lower than the inverted XY model prediction (0.67) of Dasgupta and Halperin.[3] Although the value presented here is not in agreement with theory, it is significant that it is larger than most previous results and occurred in a material characterized by a smaller value of T_{NA}/T_{NI} (see Table I). It is generally accepted that the NA transition has a tricritical point[28–30] and that for materials with sufficiently large T_{NA}/T_{NI} (small nematic ranges) the transition is first order. As the nematic range increases, the transition becomes second order and for sufficiently large nematic ranges the true critical nature of the NA transition may be observable. Therefore the larger exponent measured in 6O9 may be due in part to this effect. Unfortunately it appears that current materials may still be in the crossover region. It may be that as

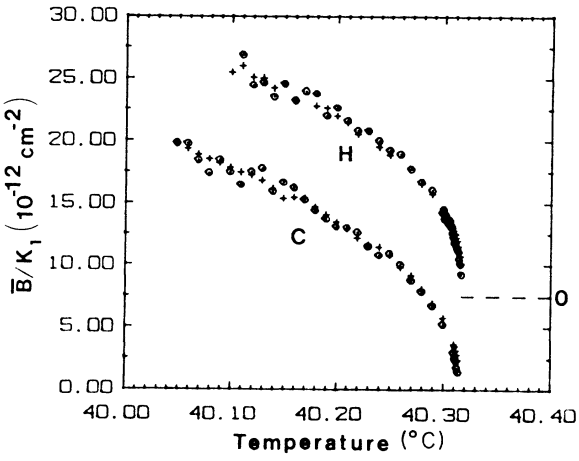

FIG. 8. $\bar{B}/K_1$ vs temperature in degrees centigrade. The data labeled with ⊙ are inverse relaxation time data. The data labeled with + are inverse intensity data. The lower two curves are from the cooling run, while the upper two curves are from the heating run. The upper curves are shifted 7.5 units.

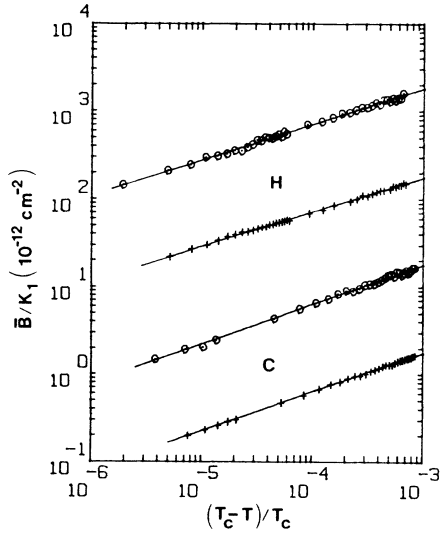

FIG. 10. Log-log plot of $\bar{B}/K_1$ vs reduced temperature. Fitted curves are drawn through each. The data have been shifted to separate the curves. The data labeled ⊙ are inverse relaxation time data. The data labeled + are inverse intensity data. The lower two curves are from the cooling run and the upper two curves are from the heating run. The upper curves have been shifted 1, 2, and 3 decades, respectively.

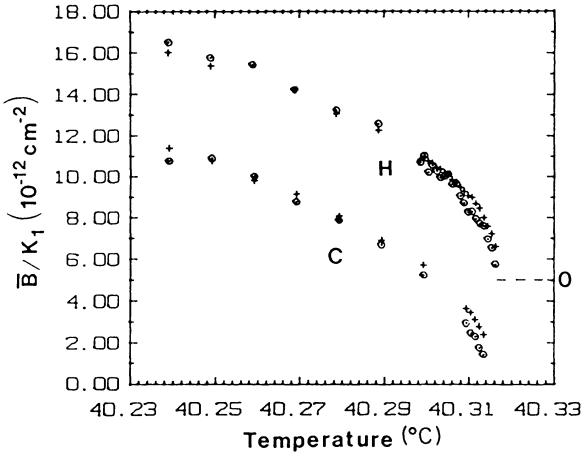

FIG. 11. Expanded plot of $\bar{B}/K_1$ vs temperature. The data have been shifted to separate the data sets. The data labeled ⊙ are inverse relaxation time data. The data labeled + are inverse intensity data. The lower two curves are from the cooling run and the upper two curves are from the heating run. The upper two curves have been shifted 5 units.

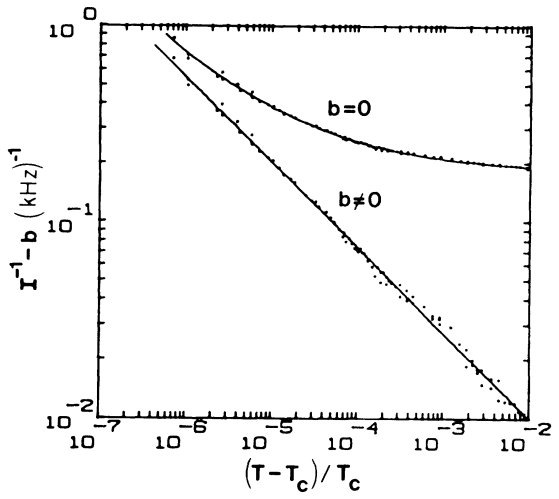

FIG. 13. Log-log plot of intensity vs reduced temperature with and without baseline. The fitted curve is also drawn.

new wider nematic range materials are studied the true critical behavior of the NA transition will be observed. Clearly much more work needs to be done in material synthesis and measurement.

The K_2 experiment.

The K_2 data were very good, covering more than four decades and giving excellent fits over this range. The parameters are stable, within the given error bars, upon range shrinking by nearly two decades. In addition, the geometric factor $F(A)$ was very stable over the entire temperature range indicating high-quality correlation data. Figure 12 is a linear plot of the intensity data while Figs. 13 and 14 are log-log plots of the I^{-1} and τI^{-1}, respectively. The measured exponents are $\rho_2=0.46\pm0.03$ (see Table I) and $\alpha_1=0.44\pm0.04$. The value of ρ_2, although larger than our previously measured values for $\bar{8}$S5 and 80CB (Table I) does not agree with the value predicted by the inverted XY model (0.67). The larger exponent may again be due in part to the larger nematic range of $\bar{6}$O9 implying that this system is further from the NA tricritical point. However, as Table I shows, the dependence of ρ_2 on T_{NA}/T_{NI} is by no means monotonic. ρ_2 was measured in a previous experiment where $q_\parallel\neq0$ and corrected for the bend contribution.[8] The corrected value is in excellent agreement with the present ($q_\parallel=0$)

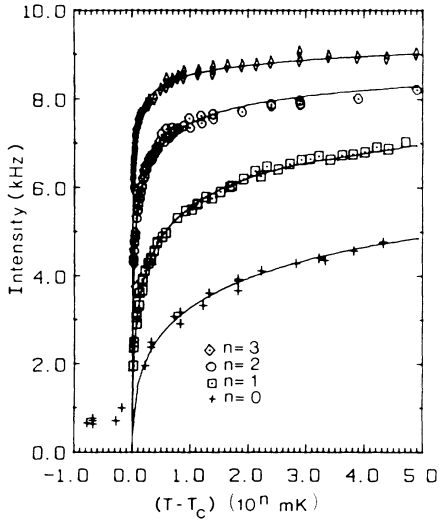

FIG. 12. Intensity vs $T-T_c$ for the mode-2 experiment. The three curves correspond to different temperature resolutions. The fitted curve is drawn through each.

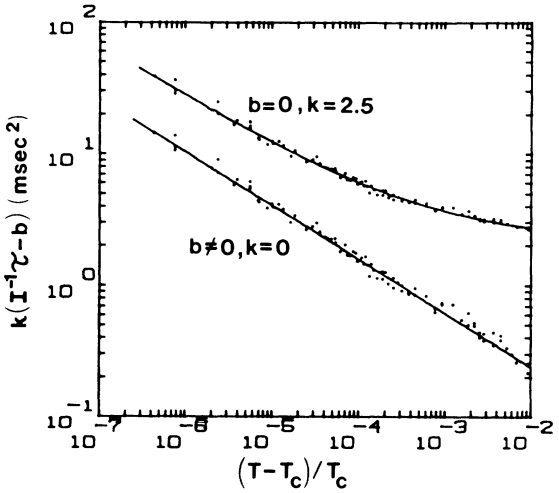

FIG. 14. Log-log plot of intensity times relaxation time vs reduced temperature with and without the baseline (b). The fitted curve is also drawn. The factor k is introduced to separate the $b=0$ and $b\neq0$ data presentations.

value (see Table I). The mode-2 viscosity exponent in the $q_{\parallel} \neq 0$ experiment was reported to be 0.46 ± 0.03.[31] The present value of 0.44 ± 0.03 is in good agreement but disagrees with the bend viscosity exponent which was reported to be $\sim \frac{1}{3}$ in agreement with the simple 3D XY theory. These exponents should be the same in the simple theory.

IV. CONCLUSIONS

From scaling it is predicted that $\phi = \rho_2$, i.e., B^{-1} and K_2 scale together. This scaling law appears to be valid for $\bar{6}O9$. It is also true that D and K_3 should scale together but the exponent for D in $\bar{6}O9$ has not yet been measured so a test of this scaling law for $\bar{6}O9$ is not possible at this time. However, results on other materials suggest that $\phi' \neq \rho_3$ (see Table I).

The results presented here are interesting and somewhat encouraging but much more work needs to be done. A thorough study of B, D, K_2, and K_3 in new materials with larger nematic ranges is needed. The results would not only allow us to rigorously test the various scaling laws but also enable us to determine if there is indeed a trend of increasing exponent with increasing nematic range. It would also be very informative to make a small-angle light scattering measurement of ρ_3 so that the exponent could be found without applying nonhydrodynamic corrections to the data,[10] enabling a direct comparison with the value obtained from Fredericks transition experiments.[9] Such experiments are currently underway on a very wide nematic range azoxybenzene material ($T_{NA}/T_{NI} = 0.87$).

ACKNOWLEDGMENTS

We want to acknowledge National Science Foundation Solid State Chemistry Program support under Grant Nos. DMR87-03524 and DMR85-15221.

[1]W. Helfrich, J. Phys. (Paris) **39**, 1199 (1978).
[2]D. R. Nelson and J. Toner, Phys. Rev. B **24**, 363 (1981).
[3]C. Dasgupta and B. Halperin, Phys. Rev. Lett. **47**, 1556 (1981).
[4]C. Dasgupta, Phys. Rev. A **27**, 1262 (1983).
[5]C. Dasgupta, Phys. Rev. Lett. **55**, 1771 (1985).
[6]P. G. de Gennes, Solid State Commun. **10**, 753 (1972).
[7]T. C. Lubensky, J. Chim. Phys. (Paris) **80**, 31 (1983).
[8]R. Mahmood, D. Brisbin, I. Khan, C. Gooden, A. Baldwi, D. L. Johnson, and M. E. Neubert, Phys. Rev. Lett. **54**, 1031 (1985).
[9]C. Gooden, R. Mahmood, D. Brisbin, A. Baldwin, D. L. Johnson, and M. E. Neubert, Phys. Rev. Lett. **54**, 1035 (1985).
[10]S. Sprunt, L. Solomon, and J. D. Litster, Phys. Rev. Lett. **53**, 1023 (1984).
[11]H. Birecki, R. Schaetzing, F. Rondelez, and J. P. Litster, Phys. Rev. Lett. **36**, 1376 (1976).
[12]F. Garcia-Golding, Ph.D. thesis, MIT, 1978.
[13]H. von Känel and J. D. Litster, Phys. Rev. A **23**, 3251 (1981).
[14]J. D. Litster, J. Als-Nielsen, R. Birgeneau, S. Dana, D. Davidov, F. Garcia-Golding, M. Kaplan, C. Safinya, and R. Schaetzing, J. Phys. (Paris) Colloq. **40**, C3-339 (1979).
[15]M. R. Fisch, P. S. Pershan, and L. B. Sorensen, Phys. Rev. A **29**, 2741 (1984).
[16]H. J. Fromm, J. Phys. **48**, 647 (1987).
[17]K. C. Chu and W. L. McMillan, Phys. Rev. A **11**, 1059 (1975).
[18]L. Cheung, R. Meyer, and H. Gruler, Phys. Rev. Lett. **31**, 349 (1973).
[19]H. Birecki and J. D. Litster, Mol. Cryst. Liq. Cryst. **42**, 33 (1977).
[20]M. Fisch, L. Sorenson, and P. Pershan, Phys. Rev. Lett. **48**, 943 (1982).
[21]C. W. Garland, M. Meichle, B. M. Ocko, A. R. Kortan, L. J. Yu, J. P. Litster, and R. J. Birgeneau, Phys. Rev. A **27**, 3234 (1983).
[22]B. M. Ocko, R. J. Birgeneau, and J. D. Litster, Phys. Rev. Lett. **52**, 108 (1984).
[23]I. Khan, Ph.D. thesis, Kent State University, 1987.
[24]M. Lewis, Ph.D. thesis, Kent State University, 1987, and this work.
[25]F. Jähnig and F. Brochard, J. Phys. (Paris) **35**, 301 (1974) (theor.); H. Birecki and J. D. Litster, Ref. 19 (expt.).
[26]M. Delaye, R. R. Ribotta, and G. Durand, Phys. Rev. Lett. **31**, 443 (1973).
[27]B. M. Ocko, Ph.D. thesis, MIT, 1984.
[28]D. Brisbin, R. DeHoff, T. Lockhart, and D. L. Johnson, Phys. Rev. Lett. **43**, 1171 (1979).
[29]J. Thoen, H. Marynissen, and W. Van Dael, Phys. Rev. Lett. **52**, 204 (1984).
[30]B. Ocko, J. Birgeneau, and L. D. Litster, Phys. Rev. Lett. **52**, 208 (1984).
[31]R. Mahmood, I. Khan, C. Gooden, A. Baldwin, and D. L. Johnson, Phys. Rev. A **32**, 1286 (1985).